Engineering 30 (2023) 93–99

Contents lists available at ScienceDirect

Engineering

journal homepage: www.elsevier.com/locate/eng

Research
Frontiers of Chemical Engineering—Letter

Ethylene Copolymerization with Linear and End-Cyclized Olefins via a Metallocene Catalyst: Polymerization Behavior and Thermal Properties of Copolymers

Changjiang Wu *, Minqiao Ren, Liping Hou, Shuzhang Qu, Xinwei Li, Cui Zheng, Jian Chen, Wei Wang *

SINOPEC (Beijing) Research Institute of Chemical Industry Co., Ltd., Beijing 100013, China

ARTICLE INFO

Article history:
Received 3 April 2023
Revised 22 May 2023
Accepted 21 July 2023
Available online 26 July 2023

Keywords:
Metallocene catalyst
Ethylene copolymerization
Comonomer distribution
Crystallization destructive capacity

ABSTRACT

Olefin solution polymerization can be used to obtain high-performance polyolefin materials that cannot be obtained via other polymerization processes. Polyolefin elastomers (POE) are a typical example. Due to cost, only a few linear α-olefins (e.g., 1-butene, 1-hexene, and 1-octene) are used as comonomers in solution polymerization in industry. However, α-olefin comonomers with other structures may have different effects on polymerization in comparison with common linear ones. Moreover, the properties of the corresponding materials may differ significantly. In this work, copolymers of ethylene with linear and end-cyclized α-olefins are synthesized using a metallocene catalyst. The copolymerization of ethylene with linear α-olefins results in a higher turn-over frequency (TOF) and lower incorporation than copolymerization with end-cyclized α-olefins, which may indicate that end-cyclized α-olefins have a higher coordination probability and lower insertion rate. In this reaction, the comonomer is distributed randomly in the polymer chain and efficiently destroys crystallization. End-cyclized α-olefins exhibit a much stronger crystallization destructive capacity (CDC) in the copolymer than linear α-olefins, possibly because linear α-olefins act mainly in the radial direction of the main chain of the polymer, while end-cyclized α-olefins act mainly in the axial direction of the main chain.

© 2023 THE AUTHORS. Published by Elsevier LTD on behalf of Chinese Academy of Engineering and Higher Education Press Limited Company. This is an open access article under the CC BY-NC-ND license (http://creativecommons.org/licenses/by-nc-nd/4.0/).

1. Introduction

Polyolefins are the most important synthetic polymer materials in daily life [1,2]. The development of olefin polymerization has been promoted by the innovation of catalysts. Compared with traditional Ziegler–Natta catalysts, single-site catalysts, including metallocene catalysts, exhibit better polymerization behavior and can endow polyolefin materials with unique structures and properties. Due to the advantages of single-site catalysts, high-density polyethylene (HDPE), medium-density polyethylene (MDPE), and linear low-density polyethylene (LLDPE) prepared via slurry and gas-phase polymerization processes have better mechanical and optical properties than the corresponding products prepared via Ziegler–Natta catalysts. However, these processes also have insurmountable defects, preventing them from giving full play to the advantages of single-site catalysts [3].

First, a single-site catalyst must be supported to meet the process requirements of slurry and gas-phase polymerization. Once a single-site catalyst is supported, it becomes a heterogeneous solid catalyst, and the uniformity of the chemical environment is damaged to a certain extent [4]. Second, due to the process characteristics of the gas phase or slurry, the comonomers used are generally limited to a few monomers with a relatively low carbon number, a low boiling point, and no heteroatoms. Third, due to process limitations, the comonomers incorporated in the polymer cannot be too high, in order to avoid production interruption due to polymer melting. Therefore, the supported single-site catalysts used in slurry and gas-phase polymerization represent a compromise between the requirements of the catalysts and the process, and the polymers obtained in this way are only an extension of the polyolefins produced using Ziegler–Natta catalysts.

In a solution polymerization system, all reaction components and the generated polymer are dissolved in a solvent. This uniform chemical environment can meet the working principles of single-site catalysts; it can also realize uniform heat and mass transfer, so that polymers with a uniform distributions of molecular weight

* Corresponding authors.
E-mail addresses: wuchangjiang.bjhy@sinopec.com (C. Wu), wangw.bjhy@sinopec.com (W. Wang).

https://doi.org/10.1016/j.eng.2023.07.001
2095-8099/© 2023 THE AUTHORS. Published by Elsevier LTD on behalf of Chinese Academy of Engineering and Higher Education Press Limited Company.
This is an open access article under the CC BY-NC-ND license (http://creativecommons.org/licenses/by-nc-nd/4.0/).

and chemical composition can actually be obtained. Moreover, due to the homogeneity of a solution system, almost any monomer can be used without considering its boiling point. Furthermore, in theory, a copolymer with any composition can be obtained without worrying about the occurrence of process accidents. Therefore, the solution polymerization process can be used to take excellent advantage of single-site catalysts in order to synthesize novel copolymers that have never been obtained before.

The most representative commercial olefin polymers obtained through solution polymerization are the polyolefin elastomers (POE). Companies that have successfully commercialized POE include ExxonMobil, Dow, Mitsui, Borealis, LyondellBasell, LG, SK, and SABIC, with a total of nearly 200 products that are widely used in impact-resistant modification, wires and cables, shoe materials, cross-linked foaming materials, vehicle materials, solar cell packaging, and so forth [5,6].

The type of comonomer used in POE, its incorporation in the polymer, and the molecular weight of the polymer determine the polymer's quality and application field. For ethylene-based POE, commonly used comonomers include propylene, 1-butene, 1-hexene, and 1-octene. Due to industry sources and costs, other monomers are rarely used [7–12].

Although the general mechanism for coordination polymerization has been well established [13,14], there are still slight differences in the polymerization processes of monomers with different structures. In particular, there are few studies on the mechanism details of less-used monomers. A difference in the mechanism results in changes in the polymerization behavior and polymer structure, which then lead to changes in the polymer properties. For example, ethylene copolymers with longer side chains exhibit different crystallization behaviors than polyethylene which has shorter branches [15]. The effect of comonomers on polymer crystallization is also well established, although this knowledge is mainly based on linear comonomers [16–18]. Thus, it is meaningful to explore the copolymerization of ethylene with comonomers that have non-traditional structures, with the aim of determining the influence of monomer structure on polymer properties, so as to guide the development of new polyolefin materials. In this work, a metallocene catalyst was used for ethylene copolymerization with comonomers having different structures, including linear α-olefins of various lengths and end-cyclized α-olefins. The influence of comonomers with different structures on the polymerization behavior and thermal properties of the polymer is discussed herein.

2. Material and methods

All experiments were carried out under a nitrogen atmosphere in a Vacuum Atmospheres dry box or using standard Schlenk techniques, unless otherwise specified. All chemicals used were of reagent grade and were purified via standard purification procedures. Toluene was distilled in the presence of sodium and benzophenone under a nitrogen atmosphere and was stored in a Schlenk tube in a dry box over molecular sieves. The metallocene catalyst $Ph_2C(Cp)(Flu)ZrCl_2$ was purchased from APAC Pharmaceutical. Methylaluminoxane (MAO) solution (10 wt% Al in toluene) was purchased from Grace and used as received. All α-olefins, including 1-hexene (C_6), 1-octene (C_8), 1-decene (C_{10}), 1-dodecene (C_{12}), 1-tetradecene (C_{14}), 1-hexadecene (C_{16}), allylcyclopentane (ACP), and allylcyclohexane (ACH), were purchased from TCI or Acros, and were used as received. Other chemicals were also used as received.

Polymerization was conducted in toluene in a 250 mL glass reactor with an oil bath at 70 °C. A glass reactor was purged with nitrogen and charged with an ethylene atmosphere (1 atm, 1 atm = 101 325 Pa). The toluene, comonomer, MAO solution, and catalyst solution in toluene were introduced in this order to start the polymerization. The mixture was stirred magnetically for 30 min. Next, the mixture was poured into EtOH (300 mL) containing HCl (10 mL). The resultant polymer was collected on filter paper via filtration, washed thoroughly with EtOH, and then dried in vacuo.

The molecular weight was determined by means of gel permeation chromatography (GPC) on a Waters Alliance GPCV2000 at 150 °C with 1,2,4-trichlorobenzene as the eluent. The melting point of the polymer was determined using TAQ 100. Approximately 2 mg of polymer sample was heated from room temperature to 160 °C with a heating rate of 10 °C per minute, under a nitrogen atmosphere. After maintaining the temperature for 1 min, the sample was cooled to room temperature with a cooling rate of 10 °C per minute to obtain the crystallization curve. Then, after maintaining the temperature for 1 min, the sample was heated to 160 °C with a heating rate of 10 °C per minute to obtain the melting curve.

Solution ^{13}C nuclear magnetic resonance (NMR) experiments were performed on a Bruker AVANCEIII-400 MHz spectrometer with a 10 mm PASEX ^{13}C–^{1}H/D Z-GRD probe. Sample solutions were prepared with approximately 250 mg of the polymer material dissolved in 2.5 mL of d_4-*o*-dichrolobenzene (ODCB-d_4) in a 10 mm tube at 130 °C. All ^{13}C NMR experiments were carried out at 125 °C, a spinning rate of 20 Hz, a pulse angle of 90°, continuous Waltz-16 decoupling, a spectral width of 120 ppm, an acquisition time of 5 s, and a relaxation delay of 10 s.

3. Results and discussion

The copolymerization of ethylene with end-cyclized α-olefins [8] or linear α-olefins with different chain lengths using similar feeding amounts was carried out with a metallocene catalyst (Fig. 1). The results are provided in Table 1.

All copolymerizations showed higher apparent activity than the homopolymerization of ethylene, due to the so-called "comonomer effect" [19]. As the structural difference between ethylene and α-olefins, a hydrogen atom on ethylene is substituted by an alkyl group to form an α-olefin comonomer. Compared with a hydrogen atom, an alkyl group has a greater electron-donating ability. From a thermodynamic perspective, this structure makes the coordination between the comonomer and the active site on the catalyst more stable than that of ethylene. After monomer insertion, the cationic active site can obtain higher electron cloud density due to the

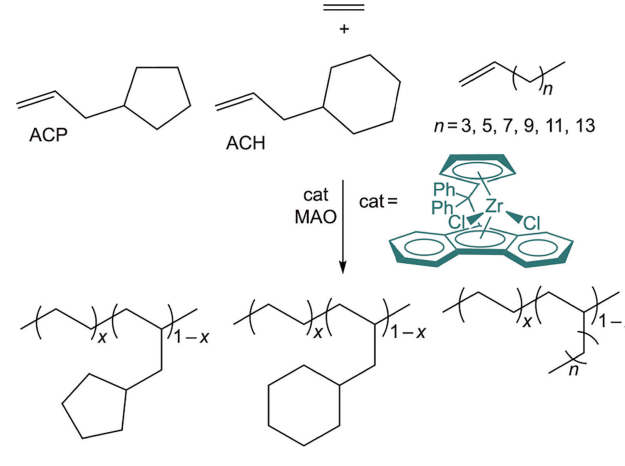

Fig. 1. Copolymerization of ethylene with end-cyclized α-olefins or linear α-olefins with various chain lengths, using a metallocene catalyst.

Table 1
Ethylene copolymerization with linear or end-cyclized α-olefins.[a]

Run	Comonomer	Feed (mmol)	Yield (g)	A (kg·(mol·h)$^{-1}$)	I_c (mol%)	T_m (°C)	ΔH (J·g^{-1})	M_n (kg·mol^{-1})	PDI	TOF (kmol·(mol·h)$^{-1}$)	NP (mol·(mol·h)$^{-1}$)	I_c/feed (mol%·mmol^{-1})	CDC
1	—	—	0.94	376	—	131	194	25.4	2.24	13.4	14.8	—	—
2	ACP	3.60	1.15	460	9.1	97	35	12.3	2.25	12.9	37.4	2.53	17.5
3	ACH	3.27	1.13	452	7.2	99	56	12.4	2.21	12.9	36.5	2.20	19.2
4	C_6	4.00	1.50	600	9.1	105	58	17.5	2.13	18.1	34.3	2.28	14.9
5	C_8	3.80	1.69	676	7.9	107	61	18.4	2.20	19.5	36.7	2.08	16.8
6	C_{10}	4.20	1.76	704	8.6	102	41	17.0	2.13	18.7	41.4	2.05	17.8
7	C_{12}	4.10	1.88	752	8.1	110	46	19.9	2.15	19.1	37.8	1.98	18.3
8	C_{14}	3.90	1.84	736	7.7	107	43	18.8	2.12	17.9	39.1	1.97	19.6
9	C_{16}	3.80	2.00	800	7.5	105	44	19.7	2.18	18.7	40.6	1.97	20.0

A: activity, in kilogram of polymer per mole of catalyst per hour; I_c: incorporation of comonomer, determined by ^{13}C NMR; T_m: melting temperature, differential scanning calorimetry (DSC) result; ΔH: melting enthalpy, DSC result; M_n: number-averaged molecular weight of the polymer, GPC result; PDI: polydispersity index, GPC result; TOF: turn-over frequency, calculated as the A divided by the molecular weight of the average monomer unit, in kilomole of monomers per mole of catalyst per hour; NP: the number of polymer chains, calculated as A/M_n, in mole of polymer chains per mole of catalyst per hour; CDC: crystallization destructive capacity of polymer, calculated as $(\Delta H_h - \Delta H_c)/I_c$, where ΔH_h and ΔH_c are the melting enthalpies of ethylene homopolymer and copolymer, respectively.
[a] $Ph_2C(Cp)(Flu)ZrCl_2$ 5 μmol, MAO 5 mmol, 70 °C, 30 min, in toluene, total 30 mL.

electron-donating group on the comonomer unit on the propagation chain, which increases the stability of the active site. These facts result in copolymerization having higher activity than ethylene homopolymerization, from a thermodynamic perspective. In addition, due to the insertion of comonomers, the crystallinity of the propagation chain is reduced, which leads to better flexibility and greater mobility of the propagation chain. As a result, the resistance of the monomer to the active site is reduced, making it possible to improve the kinetics of the polymerization activity. Therefore, introducing an alkyl-substituted comonomer into the polymerization system may improve the catalytic activity in terms of thermodynamics and kinetics.

The highest activity found in this study, that of the copolymerization of ethylene with C_{16}, is listed in Table 1. However, if the different molecular weights of each comonomer are considered, the activity presented here does not truly reflect the number of molecules engaged in the reaction. Here, the average monomer unit was defined as the mole fraction weighted average of ethylene and the comonomer. For example, the average monomer unit of sample Run 2 was $(ACP)_{0.091}(ethylene)_{0.909}$. The molecular weight of the average monomer unit (M_w) was calculated using Eq. (1). By means of the M_w, the activity can be converted to the turn-over frequency (TOF) (Eq. (2), Table 1, and Fig. 2), which can assist in providing a more realistic picture of the effect of comonomers on polymerization.

$$M_w = [M_c \times I_c + M_e \times (100 - I_c)]/100 \quad (1)$$

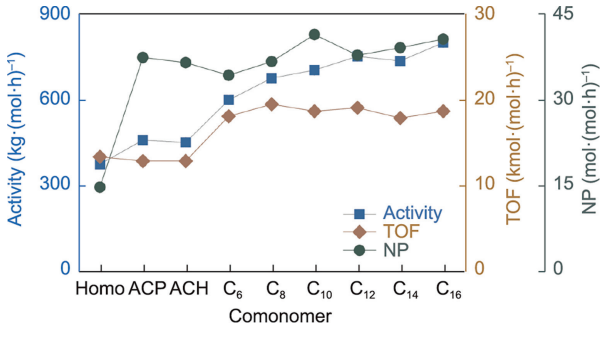

Fig. 2. Comparison of activity, TOF, and number of polymer chains (NP). The unit of activity stands for kilogram of polymer per mole of catalyst per hour; the unit of TOF stands for kilomole of monomers per mole of catalyst per hour; and the unit of NP stands for mole of polymer chains per mole of catalyst per hour. Homo: ethylene homopolymerization.

where M_c and M_e are the molecular weights of the comonomer and ethylene, respectively; and I_c is the incorporation of the comonomer. The TOF can be calculated as follows:

$$TOF = A/M_w \quad (2)$$

where A is the activity.

In fact, the TOF represents the molar activity, while the generally used term "activity" refers to the weight or mass activity. For copolymerization, the TOF can represent the "true activity" at the molecular level. It can be seen from Fig. 2 that the varied range of the TOF of the copolymerizations with linear α-olefins is much narrower than that of the activity, indicating that the molar activity of all the copolymerizations was similar, although the weight activity exhibited a relative difference. All copolymerizations with linear α-olefins exhibited a higher weight or molar activity than the ethylene homopolymerization, due to the comonomer effect on catalytic activity [19]. However, the copolymerizations with end-cyclized α-olefins had slightly lower TOFs than ethylene homopolymerization.

The generally accepted mechanism of coordination polymerization can be briefly described as follows [20]. The coordination between the monomer and the active site forms a quadrilateral intermediate containing the metal atom. The irreversible insertion of the monomer into the propagation chain and the metal atom is completed by breaking bonds (i.e., the propagation chain–metal bond and the monomer double bond) and forming bonds (i.e., the monomer unit–metal bond and the monomer unit–propagation chain bond), as illustrated in Fig. 3. The incorporation of end-cyclized monomers is comparable to that of linear olefins, indicating that the effective coordination probability of these two types of comonomers is equivalent (step 1 in Fig. 3). The TOF of the former is significantly lower than that of the latter, which may indicate that the rate of irreversible insertion of the intermediate formed by the former is lower than that of the latter (steps 2–3 in Fig. 3); that is, the intermediates of end-cyclized monomers

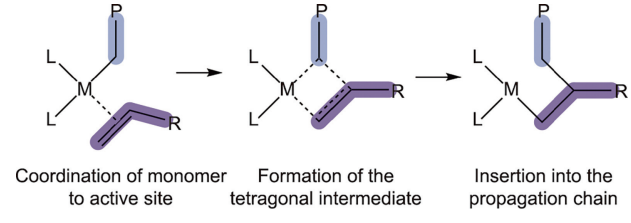

Fig. 3. The intermediate is irreversibly inserted to complete the chain growth.

have higher stability. This extra stability could come from two sources: ① The stronger electron-donating ability of end-cyclized α-olefins makes the cationic active site more stable; and ② the motion of the ring substituent may result in resistance to bonding between the monomer and the α-position carbon atom of the propagation chain.

All the polymers exhibited a narrow polydispersity index (PDI: 2.12–2.25), while the copolymer had a lower molecular weight than the polyethylene (Run 1). In particular, the copolymer of the end-cyclized α-olefins had the lowest molecular weight. Considering the low activity or TOF of the copolymerization of the end-cyclized α-olefins, the ratio of the activity to the number-averaged molecular weight (A/M_n) may be a key parameter. This ratio was calculated and is listed in Table 1, as the productivity of the number of polymer chains (NP). It was found that all copolymerizations have similar NP values (34.3–41.4 mol·(mol·h)$^{-1}$), which are significantly different from those of the homopolymerization (14.8 mol·(mol·h)$^{-1}$). From this finding, it can be argued that, if it is assumed that the efficiency of the conversion of the catalyst precursor to active sites is the same in all copolymerizations, then the same NP is produced from the active site, regardless of the comonomer and the molecular weight. However, in the case of ethylene homopolymerization, the efficiency was much lower (Fig. 2).

When the same active site is used to copolymerize different comonomers with ethylene, it produces copolymers with different chain lengths, although the time used to produce each polymer chain is the same. This finding may indicate that the active site allows an active growth chain to be attached to it for a specific amount of time. The molecular weight of the polymer at this point depends only on how rapidly the monomer is inserted. In the case of ACP or ACH, the insertion consumes a longer time and only results in a copolymer with a lower molecular weight. This result leads to an interesting conclusion: The molecular weight of the copolymer and the TOF are positively correlated. Thus, the higher the activity, the higher the molecular weight. As can be seen from Fig. 4, the performances of all the linear α-olefins are similar, and those of the two end-cycled α-olefins are also similar, yet different from those of the linear α-olefins. At the same time, the performances align with the rule that there is a positive correlation between molecular weight and TOF. However, the behavior of ethylene homopolymerization does not align with this rule.

Effective comonomer incorporation was confirmed by means of ^{13}C NMR. The end-cyclized α-olefins, ACP and ACH, gave the highest and lowest incorporation, respectively. Among the copolymerizations with linear α-olefins, the incorporation of C_6 was the highest, while that of C_{16} was the lowest. No obvious rule could be determined for the incorporation of comonomers with different structures or chain lengths, due to slight differences in the molar amount of comonomer feeding. If these differences were to be eliminated, the comonomer incorporation would exhibit a clear trend. By comparing the ratio of incorporation to the molar amount of comonomer feeding, it was found that the end-cyclized α-olefins showed a higher incorporation than the linear ones; moreover, among the linear α-olefins, monomers with a longer chain resulted in a lower incorporation. This finding may be due to the greater steric hindrance of the longer chain α-olefins (Fig. 5). When the chain reached a certain length, the influence became weak. In the case of the end-cyclized α-olefins, the end cycle can be regarded as a simple substituted group (e.g., as a "larger methyl group"), resulting in better copolymerization than 1-hexene (C_6) or 1-octene (C_8), even though ACP and ACH contain eight and nine carbon atoms, respectively.

The comonomer sequence distributions detected by means of ^{13}C NMR are summarized in Table 2. The product of the reactive ratios ($r_E r_X$, where the subscript X represents ACP, ACH, or linear comonomers, and the subscript E represents ethylene) is a representative parameter used to characterize the degree of uniformity of the distribution of copolymer monomer units within the polymer chain. Another parameter, the relative monomer dispersity (RMD) [21], developed on the basis of Hsieh and Randall's work [22], was also calculated and is listed in Table 2. We previously defined the parameter [XX]/[X] (where X represents ACP, ACH, or linear comonomers) as an evaluation of the uniformity of the distribution of the comonomer in a polymer chain [8]. The differences in these three parameters are shown in Table 3.

Because the values of the parameters, $r_E r_X$ and [XX]/[X], depend on the repeated dyad [XX], they cannot distinguish between isolated or alternative forms of comonomer. Moreover, only a copolymer with a perfectly alternative structure can achieve a maximum RMD of 200. For all copolymers that are distributed in an isolated manner in the polymer chain, the dyad is as follows:

$$\begin{cases} [EX] = a \\ [XX] = 0 \\ [EE] = 1 - a \end{cases} \tag{3}$$

Then,

$$\begin{cases} [X] = \dfrac{a}{2} \\ [E] = 1 - \dfrac{a}{2} \end{cases} \tag{4}$$

$$RMD = \frac{2}{2-a} \times 100 \tag{5}$$

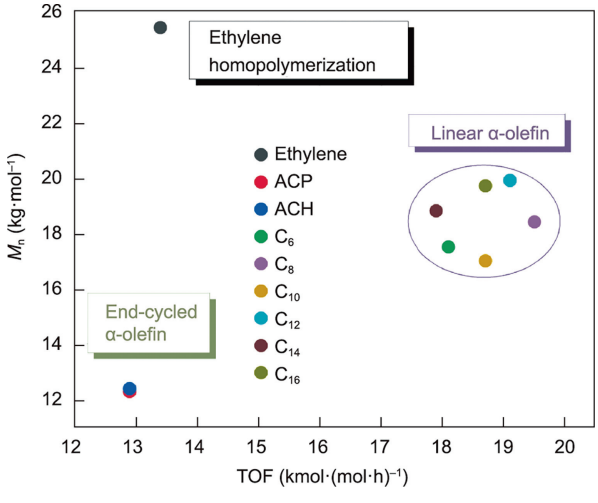

Fig. 4. Relationship between the molecular weight of the polymer and the TOF.

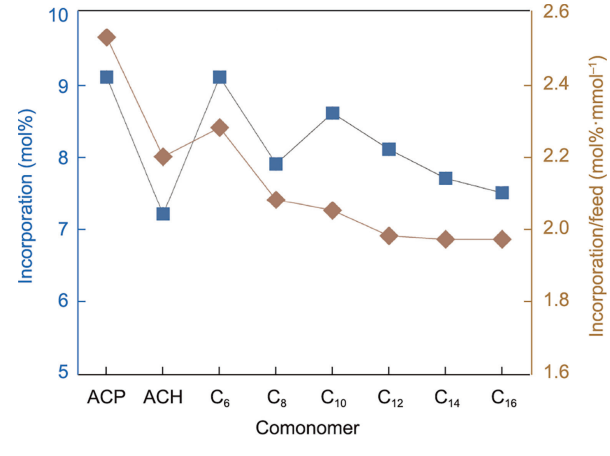

Fig. 5. Influence of comonomer structure on incorporation.

Table 2
Comonomer sequence distribution of ethylene copolymer.

Run	[XXX] (mol%)	[XXE] (mol%)	[XEX] (mol%)	[EXE] (mol%)	[XEE] (mol%)	[EEE] (mol%)	[XX] (mol%)	[EX] (mol%)	[EE] (mol%)	[X] (mol%)	[E] (mol%)	$r_E r_X$[a]	RMD (%)	[XX]/[X] (%)
2[b]	0.4	0.7	1.2	8.0	15.1	74.6	0.7	16.8	82.5	9.1	90.9	0.82	101.5	7.7
3[b]	0.1	0.8	0.8	6.4	12.0	80.0	0.5	13.5	86.0	7.2	92.8	0.94	101.0	6.9
4	0.0	0.9	1.7	8.2	13.9	75.3	0.4	17.3	82.3	9.1	90.9	0.44	104.6	4.4
5	0.0	0.8	1.4	7.0	12.1	78.8	0.4	14.8	84.8	7.8	92.2	0.62	102.9	5.1
6	0.0	0.9	1.6	7.9	13.7	75.9	0.5	16.8	82.7	8.9	91.1	0.59	103.6	5.6
7	0.0	0.9	1.5	7.2	12.3	78.1	0.5	15.3	84.2	8.1	91.9	0.72	102.8	6.2
8	0.0	0.7	1.1	7.0	12.6	78.7	0.4	14.7	85.0	7.7	92.3	0.63	103.4	5.2
9	0.0	0.8	1.2	6.7	11.8	79.6	0.4	14.2	85.5	7.5	92.5	0.68	102.3	5.3

X: ACP, ACH, or linear comonomers; E: ethylene; RMD: relative monomer dispersity, RMD = $\frac{[EX]}{2[X][E]} \times 100$.

[a] $r_E r_X = \frac{4[EE][XX]}{[EX]^2}$.

[b] The data of Runs 2 and 3 are from Ref. [8].

Table 3
The meaning, range, and corresponding microstructure of $r_E r_X$, RMD, and [XX]/[X].

Item	Calculation	Microstructure of copolymer		
		Block	Random	Alternative
$r_E r_X$	$\frac{4[EE][XX]}{[EX]^2}$	∞	1	0 (or isolated)
RMD (%)	$\frac{[EX]}{2[X][E]} \times 100$	0	100	200
[XX]/[X] (%)	$\frac{[XX]}{[X]} \times 100$	100	—	0 (or isolated)

Since $0 \leq a \leq 1$, the value of the RMD will be limited in the range of $100 \leq \text{RMD} \leq 200$. However, a microstructure with a dyad [XX] > 0 can also be located within this range. Thus, the RMD can clearly distinguish an alternate structure from isolated and random distributions, although it cannot differentiate between isolated and random distributions. The data in Table 2 shows that, for a copolymer with a low comonomer incorporation, the RMD remains at a relatively low level, although the repeated dyad is rather low. In other words, when the incorporation is low, the RMD value deviates significantly from the degree of dispersion of the comonomer. This divergence is greatly weakened when there is a high degree of incorporation. Therefore, it can be considered that the RMD is more suitable for characterizing copolymers with a high degree of incorporation, whereas [XX]/[X] is more suitable for characterizing copolymers with a low degree of incorporation, because the parameters—[XX]/[X] in particular—show the isolated distribution of the comonomer in the polymer chain in an intuitive manner.

According to the results in Table 2 and Fig. 6, all copolymerizations have an $r_E r_X$ range of 0.44–0.94 and an RMD range beyond 100, indicating that the comonomer is uniformly distributed in the polymer chain. All the values of [XX]/[X] are at a low level (less than 8), meaning that the majority of the comonomer units are isolated in the polymer chain. Unlike the linear monomers, the end-cyclized olefins give the highest product of reactive ratios and [XX]/[X], and the lowest RMD, especially ACH. This finding suggests that the copolymer structure of linear α-olefins is closer to an alternating microstructure than the copolymer structure of end-cyclized olefins, or that linear monomers tend to exist in isolation in polymer chains.

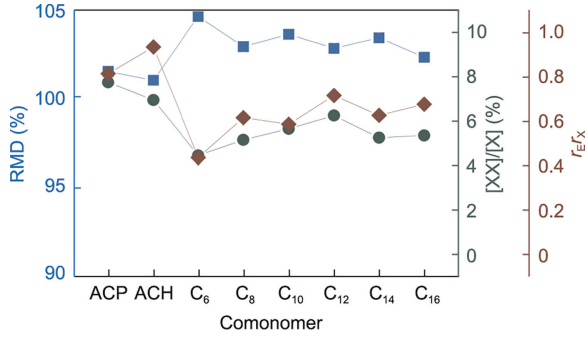

Fig. 6. Analysis of comonomer sequence distribution.

As a semi-crystallized material, polyethylene with no branches always has a crystallinity higher than 60%, according to a generally used detection method, as described in Section 2. The homopolymer in Table 1 (Run 1) has a melting enthalpy of 194 $J \cdot g^{-1}$, indicating a crystallinity of approximately 65%. The incorporation of a comonomer interrupts the successive segment of crystallizable polyethylene, and the melting point and melting enthalpy of the polymer decrease significantly. The degree of incorporation of the ACP and C_6 copolymers was observed to be the same at 9.1 mol %, although their thermal behavior differed. Fig. 7 provides the crystallization and melting curves of the two samples.

From Fig. 7(b), the broader melting range of sample Run 4 can be found, in comparison with that of sample Run 2. In addition, a melting peak near 120 °C in the differential scanning calorimetry (DSC) curve of sample Run 4 can be observed, indicating the existence of a segment with low incorporation. It can be concluded that the comonomer distribution of the ACP copolymer is broader than that of the C_6 copolymer.

For comparison, the crystallization and melting curves of all samples are provided in Fig. 8. It is easy to see that the copolymers of the two end-cyclized α-olefins have curves with a similar shape. Moreover, the copolymers obtained from linear α-olefins have the same type of curve. These observations clearly indicate that the structure of the comonomer strongly influences the thermal behavior of the copolymer.

The data in Table 1 indicate that the incorporation of all of the studied comonomers destroyed the crystallization of the polyethylene. However, the contribution of each type of comonomer remains unclear, because the structure and incorporation of the comonomers were different. Here, we define a new parameter, termed the crystallization destructive capacity (CDC) of the

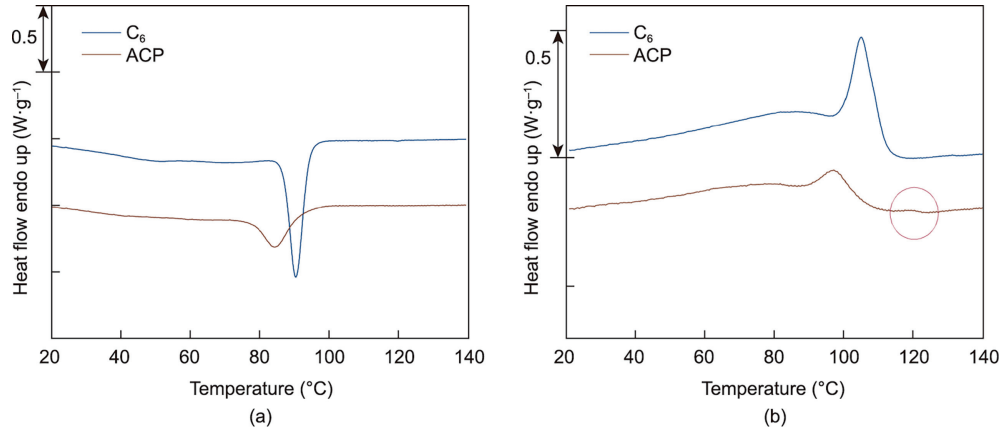

Fig. 7. (a) Crystallization and (b) melting curves of samples (Runs 2 (ACP) and 4 (C_6)) with the same copolymer incorporation (9.1 mol%). endo: endothermic.

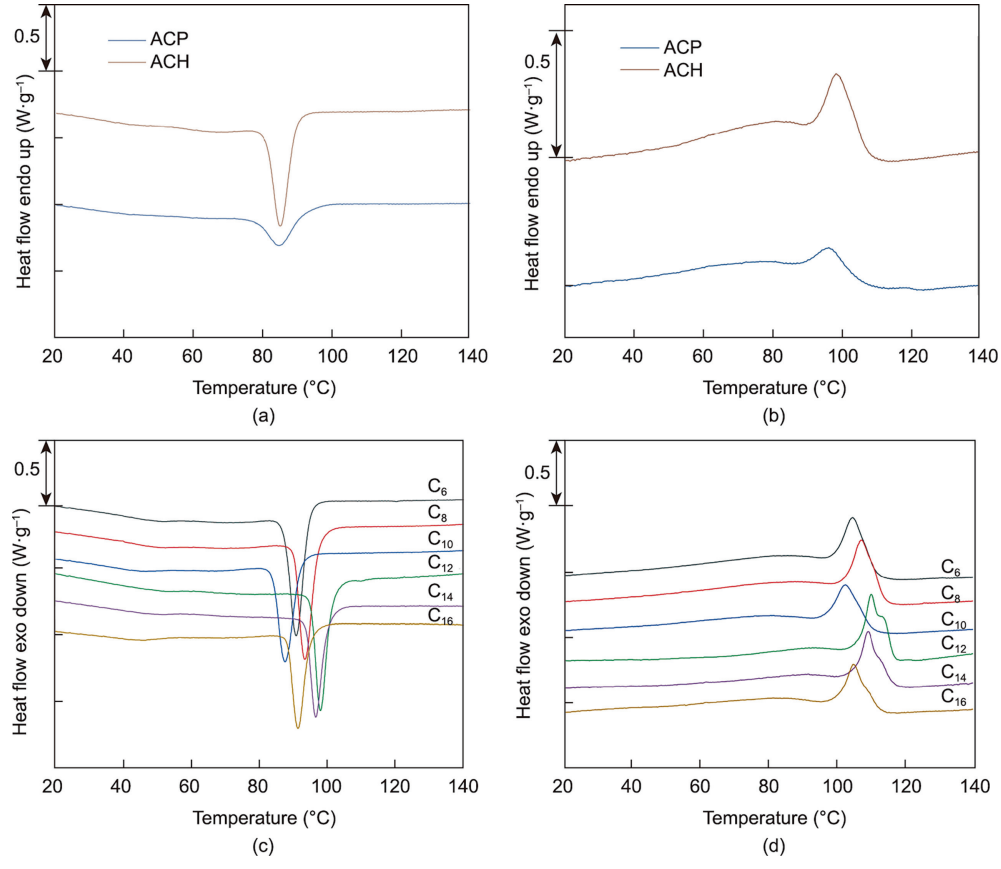

Fig. 8. (a, c) Crystallization and (b, d) melting curves of all samples. exo: exothermic.

comonomer, to eliminate the influence of comonomer incorporation and highlight the role of comonomer structure. The CDC is calculated using the followed formula:

$$\mathrm{CDC} = \frac{\Delta H_\mathrm{h} - \Delta H_\mathrm{c}}{I_\mathrm{c}} \tag{6}$$

where ΔH_h and ΔH_c are the melting enthalpies of ethylene homopolymer and copolymer, respectively; and I_c is the comonomer incorporation of each copolymer.

A clear trend is visible in the CDC of the linear α-olefins, as shown in Fig. 9. Longer comonomers have a stronger CDC, because the longer branch has a larger scope in the radial direction along (perpendicular to) the polyethylene's main chain, reducing the length of the crystallizable ethylene segment. In addition, the end-cyclized α-olefins exhibit a stronger CDC than the linear α-olefins with the same carbon numbers. It is clear that the CDC of the end-cyclized α-olefins mainly comes from the axial direction along (parallel to) the main chain. When the CH_2 segment moves to achieve the crystallization requirements, the cycloalkyl group on the side chain also moves to reach its stable conformation. These two movements are bound to interfere with each other. When the side chains are smaller and have greater motility, the crystallization process of the main chain will be more affected. From the higher CDC values of the end-cyclized α-olefins, it can

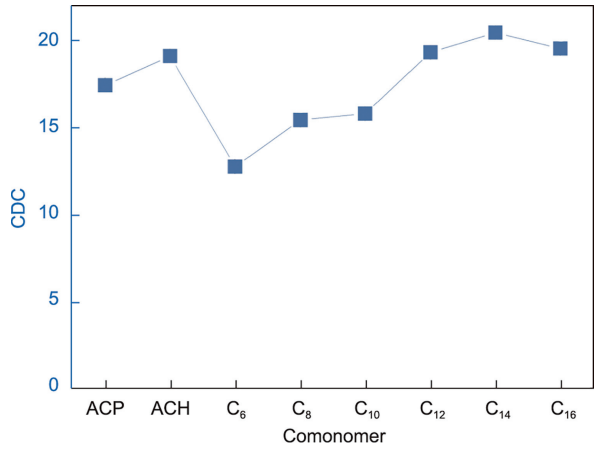

Fig. 9. A comparison of the CDC of different comonomers.

be concluded that the disturbance to the crystallization from the axial direction is much powerful than that from the radial direction.

4. Conclusions

The copolymerization of ethylene with linear α-olefins gave a higher TOF and lower incorporation of comonomers than copolymerization with end-cyclized α-olefins. This may be because end-cyclized olefins have a higher coordination probability and lower insertion rate than linear α-olefins. Copolymerization resulted in much higher polymer chain numbers than ethylene homopolymerization, which may indicate the higher coordination–insertion rate of copolymerization. Longer linear α-olefins exhibited lower copolymerization efficiency, which could be seen from the trend of the ratio of incorporation to feeding. Nevertheless, the use of end-cyclized olefins resulted in high efficiency, which may be due to the end-cyclized group behaving as a "large methyl group." This may be because the double bond of an end-cyclized α-olefin is more exposed than that of a linear α-olefin due to the ring constraint of the cyclic substituent, such that there is less steric hindrance in the coordination of an end-cyclized α-olefin with an active site, which improves the coordination probability. Moreover, a cyclic substituent may have a stronger electronic effect than a linear substituent, which can provide greater electron cloud density to the positively charged active site. The additional stability of the active site will also increase the coordination probability. However, this stability may present a higher energy barrier to further insertion reactions into the propagation chain, so the insertion rate of an end-cyclized α-olefin is lower than that of a linear α-olefin. In addition, cyclic substitution causes more methylene groups to be concentrated near the propagation chain, which may result in greater steric hindrance to the chain growth. These understandings can explain the higher incorporation and lower activity of end-cyclized α-olefins compared with linear α-olefins.

Three parameters, $r_E r_X$, RMD, and [XX]/[X], were used to characterize the microstructure of the resulting copolymer. All copolymers were randomly distributed, and most of the comonomers were isolated in the polymer chain. The incorporation of a comonomer destroyed the crystallization. Longer linear α-olefins exhibited stronger CDC than shorter ones, while end-cyclized α-olefins showed a much stronger CDC than linear ones. The reason for the latter finding may be that linear α-olefins mainly act in the radial direction of the main chain, while end-cyclized α-olefins mainly act in the axial direction of the main chain.

Compliance with ethics guidelines

Changjiang Wu, Minqiao Ren, Liping Hou, Shuzhang Qu, Xinwei Li, Cui Zheng, Jian Chen, and Wei Wang declare that they have no conflict of interest or financial conflicts to disclose.

Appendix A. Supplementary data

Supplementary material to this article can be found online at https://doi.org/10.1016/j.eng.2023.07.001.

References

[1] Gibson VC, Spitzmesser SK. Advances in non-metallocene olefin polymerization catalysis. Chem Rev 2003;103(1):283–316.
[2] Kaminsky W. Olefin polymerization catalyzed by metallocenes. Adv Catal 2001;46:89–159.
[3] Hamielec AE, Soares JBP. Polymerization reaction engineering—metallocene catalysts. Prog Polym Sci 1996;21(4):651–706.
[4] Hlatky GG. Heterogeneous single-site catalysts for olefin polymerization. Chem Rev 2000;100(4):1347–76.
[5] Mohite AS, Rajpurkar YD, More AP. Bridging the gap between rubbers and plastics: a review on thermoplastic polyolefin elastomers. Polym Bull 2022;79 (2):1309–43.
[6] Chum PS, Swogger KW. Olefin polymer technologies—history and recent progress at the Dow Chemical Company. Prog Polym Sci 2008;33(8):797–819.
[7] Zanchin G, Bertini F, Vendier L, Ricci G, Lorber C, Leone G. Copolymerization of ethylene with propylene and higher α-olefins catalyzed by (imido)vanadium (IV) dichloride complexes. Polym Chem 2019;10(45):6200–16.
[8] Wang W, Hou L, Zhang T. Integrated effect of comonomer and catalyst on copolymerization of ethylene with allylcyclopentane or allylcyclohexane by using metallocene catalysts. ChemistrySelect 2020;5(25):7581–5.
[9] Canetti M, Leone G, Ricci G, Bertini F. Structure and thermal properties of ethylene/4-methyl-1-pentene copolymers: effect of comonomer and monomer sequence distribution. Eur Polym J 2015;73:423–32.
[10] Losio S, Leone G, Bertini F, Ricci G, Sacchi MC, Boccia AC. Ethylene-4-methyl-1-pentene copolymers of complex chain architecture using α-diimine Ni(II) catalysts: synthesis, ^{13}C NMR assignment and understanding the chain-walking mechanism. Polym Chem 2014;5(6):2065–75.
[11] Xiang P, Ye Z. Copolymerization of ethylene with sterically hindered 3,3-dimethyl-1-butene using a chain-walking Pd–diimine catalyst. Macromol Rapid Commun 2010;31(12):1083–9.
[12] Losio S, Boccia AC, Boggioni L, Sacchi MC, Ferro DR. Ethene/4-methyl-1-pentene copolymers by metallocene-based catalysts: exhaustive microstructural characterization by ^{13}C NMR spectroscopy. Macromolecules 2009;42(18):6964–71.
[13] Long WP. Complexes of aluminum chloride and methylaluminum dichloride with bis-(cyclopentadienyl)-titanium dichloride as catalysts for the polymerization of ethylene. J Am Chem Soc 1959;81(20):5312–6.
[14] Cossee P. Ziegler–Natta catalysis I. Mechanism of polymerization of α-olefins with Ziegler–Natta catalysts. J Catal 1964;3(1):80–8.
[15] Kitphaitun S, Takeshita H, Nomura K. Analysis of ethylene copolymers with long-chain α-olefins (1-dodecene, 1-tetradecene, 1-hexadecene): a transition between main chain crystallization and side chain crystallization. ACS Omega 2022;7(8):6900–10.
[16] Hayatifar M, Bernazzani L, Raspolli GA. Thermal and structural investigation of random ethylene/1-hexene copolymers with high 1-hexene content. J Therm Anal Calorim 2014;115(2):1711–8.
[17] Xue Y, Bo S, Ji X. Calibration curve establishment and fractionation temperature selection of polyethylene for preparative temperature rising elution fractionation. Chin J Polym Sci 2015;33(7):1000–8.
[18] Daud M, Shehzad F, Al-Harthi MA. Crystallization behaviour and lamellar thickness distribution of metallocene-catalyzed polymer: effect of 1-alkene comonomer and branch length. Can J Chem Eng 2017;95(3):491–9.
[19] Wang W, Fan Z, Feng L, Li C. Substituent effect of bisindenyl zirconene catalyst on ethylene/1-hexene copolymerization and propylene polymerization. Eur Polym J 2005;41(1):83–9.
[20] Bochmann M. Kinetic and mechanistic aspects of metallocene polymerisation catalysts. J Organomet Chem 2004;689(24):3982–98.
[21] Wharry SM. Randomness in Ziegler–Natta olefin copolymerizations as determined by ^{13}C-NMR spectroscopy—the influence of chain heterogeneity. Polymer 2004;45(9):2985–9.
[22] Hsieh ET, Randall JC. Monomer sequence distributions in ethylene-1-hexene copolymers. Macromolecules 1982;15(5):1402–6.